

Experimental and Computational Characterization of the ^{17}O Quadrupole Coupling and Magnetic Shielding Tensors for *p*-Nitrobenzaldehyde and Formaldehyde

Gang Wu,^{*,†} Peter Mason,[†] Xin Mo,[†] and Victor Terskikh[‡]

Department of Chemistry, Queen's University, 90 Bader Lane, Kingston, Ontario, Canada K7L 3N6, and Steacie Institute for Molecular Sciences, National Research Council of Canada, Ottawa, Ontario, Canada K1A 0R6

Received: September 19, 2007; In Final Form: November 14, 2007

We have used solid-state ^{17}O NMR experiments to determine the ^{17}O quadrupole coupling (QC) tensor and chemical shift (CS) tensor for the carbonyl oxygen in *p*-nitro-[1- ^{17}O]benzaldehyde. Analyses of solid-state ^{17}O NMR spectra obtained at 11.75 and 21.15 T under both magic-angle spinning (MAS) and stationary conditions yield the magnitude and relative orientation of these two tensors: $C_Q = 10.7 \pm 0.2$ MHz, $\eta_Q = 0.45 \pm 0.10$, $\delta_{11} = 1050 \pm 10$, $\delta_{22} = 620 \pm 10$, $\delta_{33} = -35 \pm 10$, $\alpha = 90 \pm 10$, $\beta = 90 \pm 2$, $\gamma = 90 \pm 10^\circ$. The principal component of the ^{17}O CS tensor with the most shielding, δ_{33} , is perpendicular to the H–C=O plane, and the tensor component with the least shielding, δ_{11} , lies along the C=O bond. For the ^{17}O QC tensor, the largest (χ_{zz}) and smallest (χ_{xx}) components are both in the H–C=O plane being perpendicular and parallel to the C=O bond, respectively. This study represents the first time that these two fundamental ^{17}O NMR tensors have been simultaneously determined for the carbonyl oxygen of an aldehyde functional group by solid-state ^{17}O NMR. The reported experimental solid-state ^{17}O NMR results provide the first set of reliable data to allow evaluation of the effect of electron correlation on individual CS tensor components. We found that the electron correlation effect exhibits significant influence on ^{17}O chemical shielding in directions within the H–C=O plane. We have also carefully re-examined the existing experimental data on the ^{17}O spin-rotation tensor for formaldehyde and proposed a new set of best “experimental” ^{17}O chemical shielding tensor components: $\sigma_{11} = -1139 \pm 80$, $\sigma_{22} = -533 \pm 80$, $\sigma_{33} = 431 \pm 5$, and $\sigma_{\text{iso}} = -414 \pm 60$ ppm. Using this new set of data, we have evaluated the accuracy of quantum chemical calculations of the ^{17}O CS tensors for formaldehyde at the Hartree–Fock (HF), density-functional theory (DFT), Møller–Plesset second-order perturbation (MP2), and coupled-cluster singles and doubles (CCSD) levels of theory. The conclusion is that, while results from HF and DFT tend to underestimate the electron correlation effect, the MP2 method overestimates its contribution. The CCSD results are in good agreement with the experimental data.

1. Introduction

Solid-state ^{17}O NMR spectroscopy for organic and biological molecules has emerged as a new research area in recent years.^{1,2} The advantages of direct NMR detection of ^{17}O nuclei in organic and biological molecules are largely based on the remarkable sensitivity of ^{17}O NMR parameters toward molecular interactions such as hydrogen bonding and ion-carbonyl interactions. Once the practical difficulties involving NMR detection of ^{17}O nuclei in organic molecules can be overcome by utilizing ^{17}O isotopic enrichment and high magnetic fields, solid-state ^{17}O NMR spectroscopy is capable of providing new insights into chemical bonding and molecular structure. In many cases, ^{17}O NMR parameters are more sensitive to a particular type of molecular interactions than NMR parameters from other nuclei. For example, ^{17}O chemical shifts have been shown to be more sensitive than ^{13}C chemical shifts to metal–ligand interactions in carbonyl (C=O)^{3–5} and carboxyl (COO[−])^{6,7} functional groups. As part of our effort to develop solid-state ^{17}O NMR spectroscopy for biological applications, we have carried out an extensive survey of ^{17}O NMR tensors for oxygen-containing

functional groups in organic solids.^{8–16} One of our goals is to provide a baseline for understanding ^{17}O NMR tensors in organic molecules. In the past several years, several other research groups have also made significant progress in this area.^{17–39}

The aldehyde functional group (H–C=O) is important in organic chemistry. The only available data in the literature regarding ^{17}O QC and CS tensors for the carbonyl oxygen in aldehydes come from nuclear quadrupole resonance (NQR)⁴⁰ and microwave spectroscopic studies.^{41,42} To date, this important functional group has not been studied by solid-state ^{17}O NMR spectroscopy. In this study, we chose to characterize the ^{17}O NMR tensors in a simple benzaldehyde derivative, *p*-nitro-[1- ^{17}O]benzaldehyde (Figure 1), for the following reasons. First, the aldehydic oxygen atom of this compound can be readily labeled by ^{17}O . Second, high-quality crystal structures are available for this compound.^{43,44} More importantly, the crystal structure of *p*-nitrobenzaldehyde suggests that there is very little intermolecular interaction in the crystal lattice making it possible to use an isolated molecule in our computational model. Third, this compound has been previously studied by ^{17}O NQR.⁴⁰ Fourth, this molecule is relatively small allowing us to perform very high level quantum chemical calculations of NMR properties.

Another objective of this present study is to address the question as to how individual ^{17}O CS tensor components are

* Corresponding author. Phone: 613 533 2644. Fax: 1 613 533 6669. E-mail: gang.wu@chem.queensu.ca.

[†] Queen's University.

[‡] National Research Council of Canada.

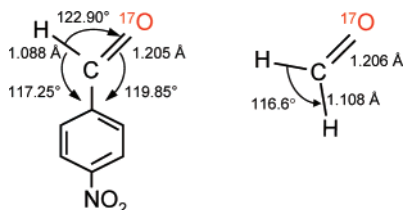


Figure 1. Chemical structures and geometric parameters of *p*-nitrobenzaldehyde and formaldehyde molecules.

affected by electron correlation. Electron correlation has been known to be important to the magnetic shielding at the ¹⁷O nucleus especially in compounds containing multiple bonds such as the C=O double bond in carbonyl compounds.⁴⁵ For example, Gauss and Stanton⁴⁶ showed that electron correlation causes a change of at least 70 ppm in the isotropic ¹⁷O chemical shift of formaldehyde. However, all previous studies have been focused on isotropic ¹⁷O chemical shifts rather than ¹⁷O CS tensor components. Once we have reliable experimental data on the ¹⁷O CS tensor in *p*-nitrobenzaldehyde, we can compare them with the results from high-level quantum chemical calculations. Because no accurate ¹⁷O CS tensor has been reported for an aldehyde oxygen, our study represents the first attempt of performing such an analysis for this important class of organic functional groups.

The final goal of this study is to re-examine the existing microwave spectroscopic data on the ¹⁷O spin-rotation tensor for formaldehyde. Because of its small size (Figure 1), formaldehyde has been used as one of the benchmark molecules to evaluate the accuracy of quantum chemical calculations for ¹⁷O chemical shielding. However, all previous studies have suffered from the simple fact that the existing ¹⁷O spin-rotation tensor data are very inaccurate. Because these spin-rotation data were used to derive the “experimental” ¹⁷O chemical shielding tensor for the carbonyl oxygen of formaldehyde in the gas phase, large uncertainties exist. For example, using the ¹⁷O spin-rotation data measured in 1965, Flygare and co-workers^{41,47,48} reported that $\sigma_{\text{iso}}(^{17}\text{O}) = -375 \pm 150$ ppm for formaldehyde. More recently, Jameson⁴⁹ used a new set of ¹⁷O spin-rotation data reported in 1980 to obtain $\sigma_{\text{iso}}(^{17}\text{O}) = -427 \pm 100$ ppm for formaldehyde. Both of these numbers have been extensively quoted in the literature. It is quite clear that, with this kind of uncertainty, it would be difficult to use them as a test for the quality of computational results. In this study, we propose a new way of constructing the best “experimental” ¹⁷O chemical shielding tensor for formaldehyde.

2. Experimental Section

Sample Preparation. Most chemicals and solvents were purchased from Sigma-Aldrich (Oakville, Ontario). The ¹⁷O labeling of *p*-nitrobenzaldehyde was achieved by dissolving 50 mg of the compound in CH₂Cl₂ and adding 0.1 mL of ¹⁷O-enriched H₂O (35% ¹⁷O atom, Cambridge Isotope Laboratories, Inc., Andover, Massachusetts). The oxygen exchange between *p*-nitrobenzaldehyde and water occurs rapidly at room temperature. The level ¹⁷O enrichment of the sample was estimated to be 30% based on solution ¹⁷O NMR measurement.

Solid-State NMR. Solid-state ¹⁷O NMR spectra of *p*-nitro-[1-¹⁷O]benzaldehyde were recorded at 11.75 and 21.15 T using Bruker Avance-500 and Bruker Avance-II 900 NMR spectrometers, respectively. For experiments with a static sample, the effective 90° pulse for the ¹⁷O central transition was 1.8 and 0.95 μs at 11.75 and 21.15 T, respectively. Magic angle spinning (MAS) spectra were obtained at 21.15 T with a 2.5 mm Bruker

MAS probe. When very fast sample spinning (>30 kHz) was employed, the sample was cooled to compensate for spinning-induced heating of the solid sample.

Quantum Mechanical Calculations. All quantum mechanical calculations were performed using Gaussian 03 software package⁵⁰ on Sun Fire 25000 servers configured with 72 × dual-core UltraSPARC-IV+1.5 GHz processors with 576 GB of RAM. SHELXTL⁵¹ was used to construct molecular models. For *p*-nitrobenzaldehyde, because the positions of hydrogen atoms were not reported, we performed a partial geometry optimization at the level of MP2/6-311G(d,p) to determine their positions. In addition, the H–C=O group exhibits a 10% disorder in the crystal lattice, the actual C=O distance used in our computation model ($R_{\text{CO}} = 1.205$ Å) is slightly different from those reported in the crystallographic studies ($R_{\text{CO}} = 1.204$ Å for the major conformer⁴³ and $R_{\text{CO}} = 1.197$ and 1.256 Å for the major and minor conformers, respectively⁴⁴). Because there is little intermolecular interaction in the crystal lattice of *p*-nitrobenzaldehyde, we used an isolated molecule in our computations. For formaldehyde, the experimental structure of Oka⁵² was used in the model as shown in Figure 1. The principal components of the electric field gradient (EFG) tensor, q_{ii} ($ii = xx, yy, zz$; $|q_{zz}| > |q_{yy}| > |q_{xx}|$ and $q_{zz} + q_{yy} + q_{xx} = 0$), were computed in atomic units (1 au = 9.717365×10^{21} V m⁻²). The principal magnetic shielding tensor components (σ_{ii}) were computed with $\sigma_{\text{iso}} = (\sigma_{11} + \sigma_{22} + \sigma_{33})/3$ and $\sigma_{33} > \sigma_{22} > \sigma_{11}$. In solid-state NMR experiments, the measurable quantities for a quadrupole coupling tensor are the quadrupole coupling constant (C_Q) and the asymmetry parameter (η_Q). To compare calculated results with experimental NMR parameters, following equations were used:

$$C_Q[\text{MHz}] = e^2 q_{zz} Q/h = -243.96 \times Q[\text{barn}] \times q_{zz}[\text{au}] \quad (1)$$

$$\eta_Q = (q_{xx} - q_{yy})/q_{zz} \quad (2)$$

where Q is the nuclear quadrupole moment, e is the elementary charge, and h is the Planck constant. Typically, the standard value⁵³ for $Q(^{17}\text{O})$, -2.558×10^{-30} m², was used, except cases mentioned in the text. To make direct comparison between the calculated chemical shielding, σ , and the observed chemical shift, δ , we used the new absolute ¹⁷O chemical shielding scale reported by Wasylishen and Bryce⁵⁴

$$\delta (\text{ppm}) = 287.5 (\text{ppm}) - \sigma (\text{ppm}) \quad (3)$$

3. Results and Discussion

Analysis of ¹⁷O MAS NMR Spectra. Figure 2 shows the ¹⁷O MAS NMR spectra of *p*-nitro-[1-¹⁷O]benzaldehyde at 21.15 T. It can be seen immediately that each MAS spectrum spans a range of over 1000 ppm, indicating the presence of large ¹⁷O chemical shift anisotropy (CSA) for the aldehyde oxygen atom. The fact that the total width of the individual spinning sidebands is on the order of 12 kHz at 21.15 T is in agreement with the expectation from ¹⁷O NQR result for a C_Q value of greater than 10 MHz.⁴⁰ Also shown in Figure 2 are the numerical simulations of the spinning sidebands. However, it should be mentioned that these simulations were performed only after the ¹⁷O NMR tensor parameters had been extracted from an analysis of static ¹⁷O NMR spectra (vide infra). As we have illustrated previously,⁹ a general approach of analyzing solid-state ¹⁷O NMR spectra is to start from the MAS spectrum (if available). In the present case, however, because of the presence of many spinning sidebands, none of the individual spinning sidebands exhibits a

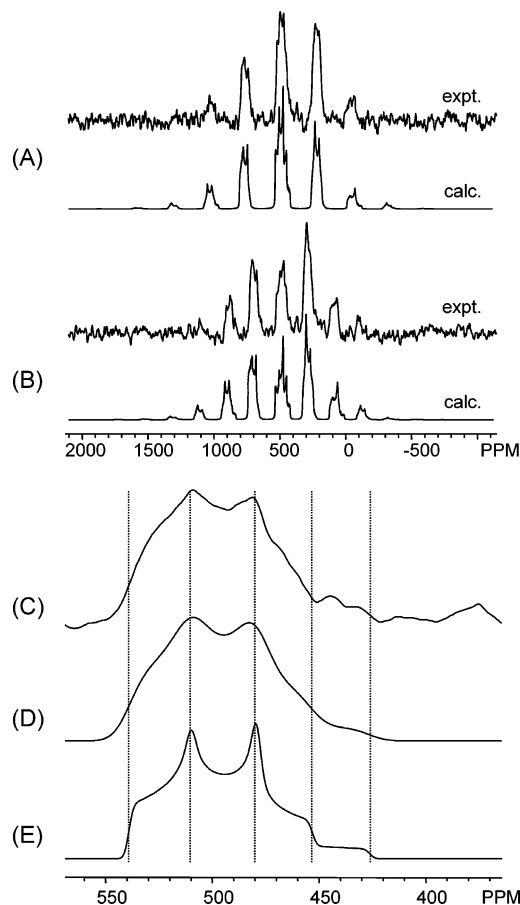


Figure 2. (A, B) Experimental (upper trace) and calculated (lower trace) ^{17}O MAS spectra of *p*-nitro-[1- ^{17}O]benzaldehyde obtained at 21.15 T. Detailed experimental parameters are as follows: (A), 33 kHz MAS, 2048 transients, 5 s recycle delay; (B), 25 kHz MAS, 4914 transients, 5 s recycle delay. (C) The total line shape by adding all spinning sidebands in (B). Simulated ^{17}O MAS spectra of *p*-nitro-[1- ^{17}O]benzaldehyde (D) with 1.6 kHz line broadening and (E) without line broadening.

complete line shape from which a theoretical analysis can be performed. Under such a circumstance, one must add all spinning sidebands together to produce a complete line shape as illustrated in Figure 2. Comparison with the theoretical line shape yields the following ^{17}O NMR parameters: $\delta_{\text{iso}} = 545 \pm 5$ ppm, $C_Q = 10.7 \pm 0.2$ MHz, and $\eta_Q = 0.45 \pm 0.10$. Our ^{17}O quadrupole parameters are in good agreement with the ^{17}O NQR data obtained at 77 K: $C_Q = 10.6$ MHz and $\eta_Q = 0.45$.⁴⁰ The isotropic ^{17}O chemical shift of *p*-nitrobenzaldehyde in the solid state is somewhat different from that measured in $\text{CD}_3\text{-CN}$ solution for the same compound, $\delta = 587$ ppm. This is not so surprising, because large solvent-induced shifts are quite common in ^{17}O NMR of organic compounds.

Analysis of Static ^{17}O NMR Spectra. After obtaining the values of δ_{iso} , C_Q , and η_Q from an analysis of MAS spectra, we now can analyze static ^{17}O NMR spectra in order to get the remaining information about the ^{17}O CS tensor components and the relative orientation of the QC and CS tensors. Figure 3 shows the static ^{17}O NMR spectra of *p*-nitrobenzaldehyde obtained at 11.75 and 21.15 T, together with the spectral simulations. It is noted that the total width of the spectrum exceeds 120 and 145 kHz at 11.75 and 21.15 T, respectively. This immediately suggests that ^{17}O chemical shift anisotropy is an important contributor to the total spectral width. We will examine the interplay between the ^{17}O QC and CS tensors in the next section. Here these high-quality ^{17}O NMR spectra allow us to extract

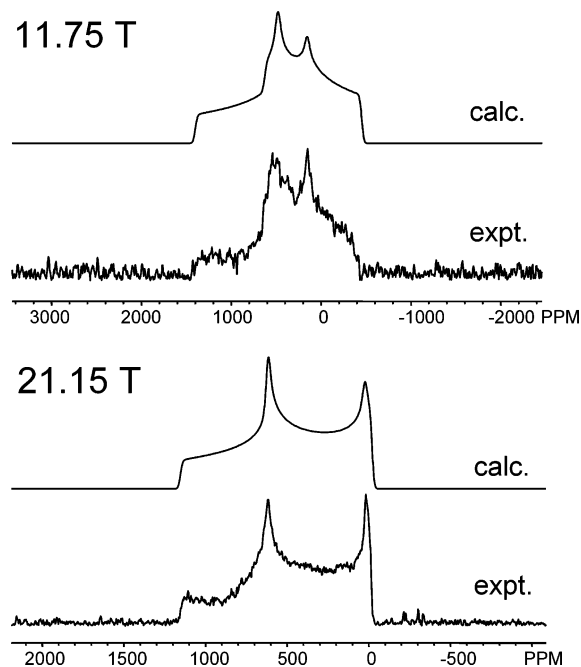


Figure 3. Experimental (upper trace) and simulated (lower trace) static ^{17}O NMR spectra of *p*-nitro-[1- ^{17}O]benzaldehyde. The experimental parameters are as follows: 11.75 T, 0.4 MHz spectral window, 10 s recycle delay, 8918 transients, 70 kHz ^1H decoupling field; 21.15 T, 0.4 MHz spectral window, 5 s recycle delay, and 17397 transients, 100 kHz ^1H decoupling field. Whole-echo detection with an inter-pulse delay of 60 μs was used for collecting data at both fields.

accurate data about the ^{17}O CS tensor: $\delta_{11} = 1050 \pm 10$, $\delta_{22} = 620 \pm 10$, $\delta_{33} = -35 \pm 10$ ppm, $\alpha = 90 \pm 10^\circ$, $\beta = 90 \pm 2^\circ$, and $\gamma = 90 \pm 10^\circ$. This represents the first reliable ^{17}O CS tensor characterization for the carbonyl oxygen from an aldehyde group. The relative orientation between the ^{17}O QC and CS tensors is such that the CS tensor component with the least shielding, δ_{11} , coincides with the smallest QC tensor component, χ_{xx} , whereas the intermediate CS tensor component, δ_{22} , lies along the direction of the largest QC tensor component, χ_{zz} . Of course, our spectral analysis yields only the relative tensor orientation between the two tensors; the absolute tensor orientation in the molecular frame can be obtained from quantum chemical calculations, as will be discussed in a later section.

Interplay of ^{17}O QC and CS Tensors. As mentioned earlier, the total line width (measured in Hertz) of the static ^{17}O NMR spectrum of *p*-nitrobenzaldehyde obtained at 21.15 T is greater than that at 11.75 T. In this section, we examine the influence of interplay between ^{17}O QC and CS tensors on the total spectral width for an aldehyde oxygen. Figure 4 shows the theoretical ^{17}O NMR spectra for an aldehyde oxygen subject to various nuclear spin interactions: a pure ^{17}O QC tensor, a pure ^{17}O CS tensor and both of the two tensors. It is well-known that the line width contribution from second-order quadrupole and chemical shielding interactions is inversely proportional and directly proportional to the applied magnetic field, respectively. The consequence of these two opposing factors is that the total line width of an ^{17}O NMR spectrum does not always decrease with the increase of the applied magnetic field strength. As seen in Figure 5, the total line width reaches a minimum at around 12.5 T for *p*-nitrobenzaldehyde. At 11.75 T, the contributions from QC and CS tensors are approximately equal, whereas at 21.15 T the CS tensor dominates the total line width. It should be pointed out that the exact field dependence of the line width depends also on the relative orientation between the two tensors. Nonetheless, the case of *p*-nitrobenzaldehyde illustrates that the

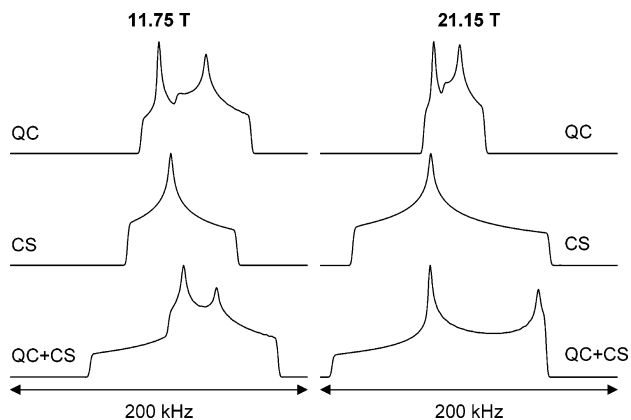


Figure 4. Illustration of the interplay between ^{17}O QC and CS tensors for *p*-nitrobenzaldehyde at two magnetic fields.

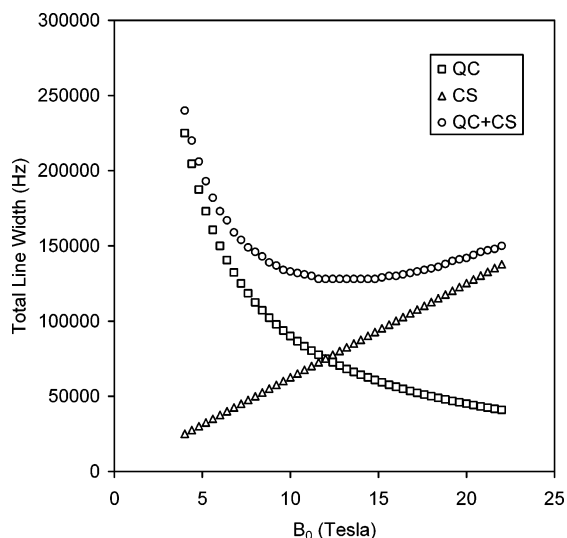


Figure 5. Dependence of the total ^{17}O NMR line width for a stationary powder sample on the strength of the applied magnetic field. Experimental ^{17}O NMR parameters for *p*-nitrobenzaldehyde were used in the calculation.

interplay of the two ^{17}O NMR tensors has a significant effect on the total spectral width. This is also an example to emphasize the importance of obtaining solid-state ^{17}O NMR data at multiple magnetic fields in order to determine the two tensors simultaneously.

^{17}O NMR Tensors in Carbonyl Compounds. In this section we compare the solid-state ^{17}O NMR results for the carbonyl oxygen of aldehydes with those of other carbonyl compounds such as ketone, amide, and urea functional groups. Here we chose *p*-nitrobenzaldehyde, benzophenone, benzamide and urea as representative carbonyl compounds for comparison. The ^{17}O QC and CS tensor orientations for these carbonyl compounds are illustrated in Figure 6. Benzophenone is the only ketone compound for which ^{17}O NMR tensors have been determined experimentally.⁵⁵ For benzophenone, the ^{17}O CS and QC tensor orientations are identical to those observed for *p*-nitrobenzaldehyde. For primary and secondary amides, Wu and co-workers^{8,9} reported the orientations of the ^{17}O NMR tensors. Figure 6 shows the ^{17}O NMR tensors of benzamide as an example for amides. Although the ^{17}O CS tensor for benzamide has the same orientation as those of aldehydes and ketones, the ^{17}O QC tensor exhibits a discrepancy. In particular, the smallest ^{17}O QC tensor component, χ_{xx} , is now perpendicular to the H–C=O plane and the intermediate component, χ_{yy} , is along the C=O bond. The ^{17}O NMR tensors in crystalline urea have

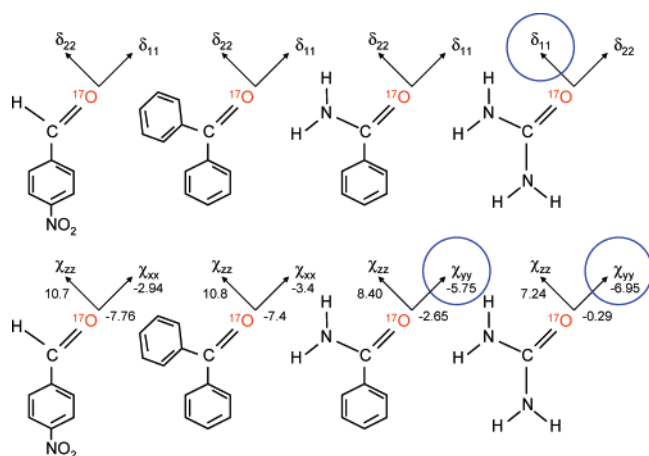


Figure 6. Schematic diagrams showing the ^{17}O QC (below) and CS (above) tensor orientations in the molecular frame of reference for several carbonyl compounds: *p*-nitrobenzaldehyde, benzophenone, benzamide, and urea. The blue circles highlight the discrepancy in tensor orientations. Tensor components perpendicular to the plane are not shown for clarity.

also been determined by Wu and co-workers.¹⁰ For urea, the ^{17}O QC tensor has the same orientation as that of benzamide, but the ^{17}O CS tensor differs. That is, the direction of δ_{11} is now perpendicular to the C=O bond. For the ^{17}O QC tensor, two general trends are observed for these carbonyl compounds. First, although the magnitude of C_Q decreases from *p*-nitrobenzaldehyde (10.7 MHz) and benzophenone (10.8 MHz) to benzamide (8.4 MHz) and to urea (7.2 MHz), the direction of the largest QC tensor component, χ_{zz} , is always in-plane and perpendicular to the C=O bond. Second, the direction switch of χ_{xx} and χ_{yy} components between *p*-nitrobenzaldehyde/benzophenone and benzamide/urea results from a combined effect from simultaneous increase and decrease of EFG along and perpendicular (out-of-the-plane) to the C=O bond, respectively. When the magnitudes of EFG along these two directions get closer, η_Q approaches zero. Further changes would then result in a switch of χ_{xx} and χ_{yy} components because the definition of χ_{xx} and χ_{yy} components depends on their relative magnitudes (i.e., $|\chi_{xx}| < |\chi_{yy}|$). This switch of χ_{xx} and χ_{yy} components has been discussed in details by Gready^{56,57} on the basis of experimental ^{17}O NQR results and computational data. For the ^{17}O CS tensor, the tensor orientations are the same in these four carbonyl compounds, except for a switch in the directions of δ_{11} and δ_{22} components in urea. This δ_{11} – δ_{22} switch in crystalline urea was discussed extensively by Wu and co-workers.¹⁰ Clearly, this switch occurs because the paramagnetic shielding contribution from the $n \rightarrow \pi^*$ mixing no longer dominates the ^{17}O chemical shielding in urea. Urea is the first carbonyl compound (and the only one to date) where δ_{11} is found to be perpendicular to the C=O bond.

Among the carbonyl compounds, we found a correlation between the value of C_Q and the ^{17}O CS tensor components, as depicted in Figure 7 where we have also included solid-state ^{17}O NMR data from other carbonyl compounds such as nucleic acid bases^{5,16} and peptides.^{4,34} A general trend is that both C_Q (^{17}O) and $\delta_{\text{iso}}(^{17}\text{O})$ increase with the C=O π bond order. Cheng and Brown⁴⁰ first noted this trend in their early NQR studies. Here our examination of individual ^{17}O chemical shift tensor components reveals more insights into the origin of this correlation. As seen in Figure 7, the correlation between C_Q (^{17}O) and $\delta_{\text{iso}}(^{17}\text{O})$ arises mainly from the δ_{11} and δ_{22} components, suggesting that the paramagnetic contribution to chemical shielding must be responsible for such a correlation. It is also

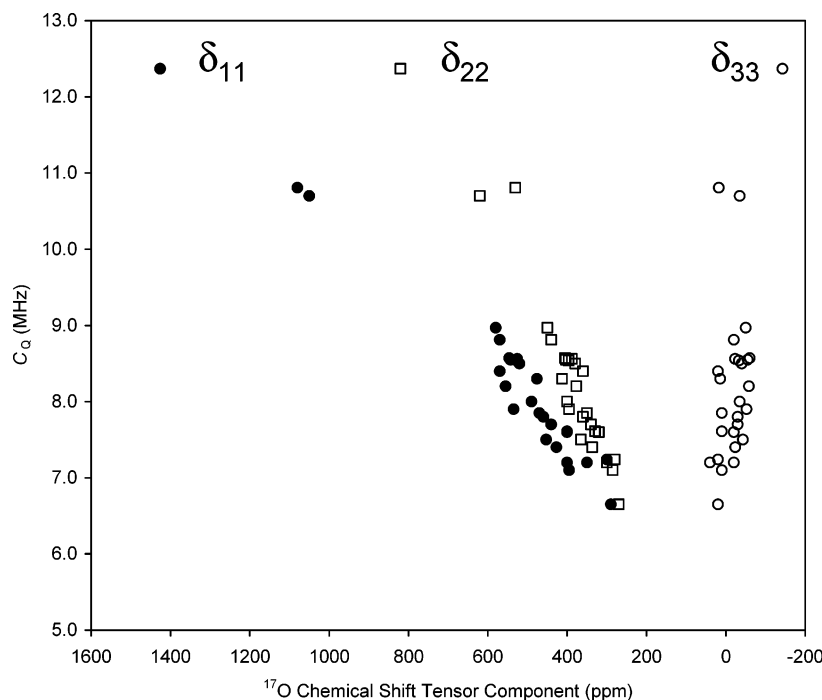


Figure 7. Correlation between the ^{17}O quadrupole coupling constant and ^{17}O CS tensor components for carbonyl compounds.

TABLE 1: Computed and Experimental ^{17}O QC and CS Tensors for the Carbonyl Oxygen of *p*-Nitrobenzaldehyde^a

method/basis set	δ_{iso} (ppm)	δ_{11} (ppm)	δ_{22} (ppm)	δ_{33} (ppm)	C_Q (MHz) ^b	C_Q (MHz) ^c	η_Q
HF/6-31G	698.5	1394.4	832.8	-131.7	13.626	12.145	0.465
6-311G	744.3	1473.1	879.8	-119.9	14.286	12.729	0.475
6-311G(d,p)	597.7	1182.8	734.5	-124.3	12.454	11.096	0.491
cc-pVDZ	615.1	1217.4	748.4	-120.5	9.558	8.516	0.643
cc-pVTZ	631.1	1231.9	778.1	-116.8	10.118	9.015	0.584
cc-pVQZ	635.5	1243.0	782.2	-118.8	12.801	11.406	0.594
B3LYP/6-31G	641.5	1312.8	712.7	-100.8	12.357	11.591	0.457
6-311G	703.6	1416.5	778.0	-83.6	13.133	12.319	0.501
6-311G(d,p)	589.0	1191.1	672.6	-96.5	11.485	10.773	0.499
cc-pVDZ	608.2	1229.5	685.8	-90.6	8.844	8.296	0.652
cc-pVTZ	636.0	1267.4	728.3	-87.7	9.543	8.951	0.581
cc-pVQZ	644.1	1285.9	736.4	-89.9	12.001	11.257	0.617
MP2/6-31G	698.5	1394.4	832.8	-131.7	13.649	12.584	0.470
6-311G	540.8	1110.9	617.8	-106.3	14.316	13.199	0.480
6-311G(d,p)	475.8	983.7	559.3	-115.6	12.478	11.505	0.496
cc-pVDZ	615.1	1217.3	748.4	-120.5	12.742	11.748	0.508
cc-pVTZ	540.4	1098.3	631.3	-108.4	12.705	11.714	0.602
cc-pVQZ	505.7 ^d	1025.3 ^d	608.1 ^d	-116.4 ^d	12.835	11.830	0.598
exptl.	545 ± 5	1050 ± 10	620 ± 10	-35 ± 10		10.7 ± 0.2	0.45 ± 0.10

^a The GIAO method was used in chemical shielding calculations. ^b Calculated using the standard value of $Q(^{17}\text{O})$, -2.558 fm^2 . ^c Calculated using the calibrated values of $Q(^{17}\text{O})$: HF, -2.28 ; B3LYP, -2.40 ; MP2, -2.36 fm^2 . For calibrated $Q(^{17}\text{O})$ values, see ref 2. ^d Calculated using a locally dense basis set: cc-pVQZ for oxygen and 6-31G(d,p) for other atoms.

remarkable to note that the change of δ_{11} for these organic carbonyl compounds is greater than 1100 ppm! The large spans of the ^{17}O CS tensors found for formaldehyde and *p*-nitrobenzaldehyde are due to the small $n \rightarrow \pi^*$ energy gaps in these compounds.

Quantum Chemical Calculations. Because we have obtained accurate ^{17}O NMR tensor components for an aldehyde oxygen group, it is now possible to evaluate the accuracy of quantum chemical calculations. The primary objective here is to examine the influence of electron correlation on individual ^{17}O CS tensor components rather than the isotropic value alone. We have performed extensive quantum chemical calculations for the ^{17}O QC and CS tensors of *p*-nitrobenzaldehyde using HF, B3LYP and MP2 methods. The computational results are summarized in Table 1. All calculations predict $\alpha = \beta = \gamma =$

90° between the ^{17}O QC and CS tensors, in excellent agreement with the experimental results. In general, HF and B3LYP results on δ_{11} and δ_{22} of the ^{17}O CS tensor are very similar and considerably higher than the experimental values. In contrast, MP2 calculations with large basis sets such as cc-pVTZ and cc-pVQZ seem to show a better convergence and the results are in much better agreement with the experimental data. All three methods yield δ_{33} values consistently more shielded than the experimental value by 50–80 ppm (ca. 11–18% on the absolute shielding scale). It is unclear at this time as to the origin of this discrepancy.

Because it is computationally demanding to use MP2 and large basis sets even for a small molecule like *p*-nitrobenzaldehyde, we performed more MP2 computations using locally dense basis sets. The detailed computational results are given

as Supporting Information. It is clear that both ¹⁷O CS and QC tensors exhibit convergence so there is no additional benefit to use basis sets beyond cc-pVTZ. We also explored other methods for shielding calculations as implemented in Gaussian 03: single gauge origin (SGO), individual gauges for atoms in molecules (IGAIM), and continuous set of gauge transformations (CSGT).^{58–60} Our computational results suggest that all these computational methods produce comparable results (see the Supporting Information).

Evaluation of the ¹⁷O CS Tensor in Formaldehyde. Now we have developed a general sense regarding to the relationship between ¹⁷O CS tensor components and electron correlation for an aldehyde oxygen. Here we extend our approach to examine the ¹⁷O NMR tensors for formaldehyde. As mentioned earlier, Flygare and co-workers^{41,47,48} and Jameson⁴⁹ have reported conversion of the experimental ¹⁷O spin-rotation data to the “experimental” ¹⁷O CS tensor for formaldehyde. The relationship between spin rotation constants and paramagnetic nuclear shielding was established by Ramsey⁶¹ and Flygare.⁶² The paramagnetic shielding tensor components (σ_{ii}^p , $ii = xx, yy, zz$) are related to the spin-rotation tensor components (M_{ii} , $ii = xx, yy, zz$) in the following fashion:

$$\sigma_{xx}^p = \frac{m_p}{2mg_N} \frac{M_{xx}}{A} - \frac{\mu_0}{4\pi} \frac{e^2}{2m} \sum_N \frac{Z_N}{R_N^3} (y_N^2 + z_N^2) \quad (4)$$

$$\sigma_{yy}^p = \frac{m_p}{2mg_N} \frac{M_{yy}}{B} - \frac{\mu_0}{4\pi} \frac{e^2}{2m} \sum_N \frac{Z_N}{R_N^3} (x_N^2 + z_N^2) \quad (5)$$

$$\sigma_{zz}^p = \frac{m_p}{2mg_N} \frac{M_{zz}}{C} - \frac{\mu_0}{4\pi} \frac{e^2}{2m} \sum_N \frac{Z_N}{R_N^3} (x_N^2 + y_N^2) \quad (6)$$

where m_p is the proton mass, g_N is the nuclear g -factor ($g_N = -0.75752$ for ¹⁷O),⁶³ m is the electron mass, e is the elementary charge, A , B , and C are the rotational constants, (x_N, y_N, z_N) are the Cartesian coordinates of the N th nucleus with the nucleus of interest as the gauge origin, and R_N is the distance between the N th nucleus and the nucleus of interest. The summation in the above equations goes over all the other nuclei in the molecule. According to Ramsey formalism, the second contribution to the total chemical (magnetic) shielding at the nuclear position is the diamagnetic shielding, whose principal tensor components (σ_{ii}^d , $ii = xx, yy, zz$) are expressed as

$$\sigma_{xx}^d = \frac{\mu_0}{4\pi} \frac{e^2}{2m} \langle \psi^0 | (y_N^2 + z_N^2)/R_N^3 | \psi^0 \rangle \quad (7)$$

$$\sigma_{yy}^d = \frac{\mu_0}{4\pi} \frac{e^2}{2m} \langle \psi^0 | (x_N^2 + z_N^2)/R_N^3 | \psi^0 \rangle \quad (8)$$

$$\sigma_{zz}^d = \frac{\mu_0}{4\pi} \frac{e^2}{2m} \langle \psi^0 | (x_N^2 + y_N^2)/R_N^3 | \psi^0 \rangle \quad (9)$$

where ψ^0 is the ground-state wavefunction of the molecular system. The diamagnetic shielding tensor can be readily calculated to high accuracy because it depends only on the ground-state wavefunction of the molecule. Therefore, the general approach to derive chemical shielding tensor components is first to obtain σ_{ii}^p from experimental results for M_{ii} , A , B and,

TABLE 2: Principal Components of the ¹⁷O Spin-Rotation Tensor, Rotational Constants, and Principal Components of the ¹⁷O Chemical Shielding Tensor (in ppm) for Formaldehyde

	Flygare ³⁶	Jameson ³⁷	this work
M_{xx} (kHz)	371 ± 10	361.1 ± 21.9	361.1 ± 21.9
M_{yy} (kHz)	25 ± 10	28.6 ± 3.0	28.6 ± 3.0
M_{zz} (kHz)	-2 ± 10	0	(-0.8) ^a
A (GHz)	282.0290	281.9650	281.9650
B (GHz)	38.83528	37.812287	37.812287
C (GHz)	34.00316	33.214523	33.214523
σ_{xx} (diamagnetic)	418	415.81	415.8
σ_{yy} (diamagnetic)	468	465.15	465.1
σ_{zz} (diamagnetic)	470	475.13	475.1
σ_{ave} (diamagnetic)	452	452.03	452.0
σ_{xx} (paramagnetic)	-1600 ± 50	-1555 ± 95	-1555 ± 80
σ_{yy} (paramagnetic)	-870 ± 300	-998 ± 96	-998 ± 80
σ_{zz} (paramagnetic)	-10 ± 100	-84 ± 100	(-44) ^a
σ_{xx} (total)	-1182 ± 50	-1139 ± 100	-1139 ± 80
σ_{yy} (total)	-402 ± 300	-533 ± 100	-533 ± 80
σ_{zz} (total)	460 ± 100	391 ± 100	431 ± 5
σ_{iso} (total)	-375 ± 150	-427 ± 100	-414 ± 60

^a See text for discussion.

C , and molecular geometry using eqs 4–6, then to couple it with theoretical results for σ_{ii}^d , because if one is only interested

$$\sigma_{ii}^{total} = \sigma_{ii}^p + \sigma_{ii}^d \quad (10)$$

in the isotropic chemical shielding constant, $\sigma_{iso} = (\sigma_{xx} + \sigma_{yy} + \sigma_{zz})/3$, the following equation holds within a few parts per million⁴⁷

$$\sigma_{iso} \approx \sigma(\text{free atom}) + \frac{m_p}{2mg_N} \frac{1}{3} \left(\frac{M_{xx}}{A} + \frac{M_{yy}}{B} + \frac{M_{zz}}{C} \right) \quad (11)$$

As shown in Table 2, Flygare and co-workers^{41,47,48} and Jameson⁴⁹ used the aforementioned method to obtain the ¹⁷O chemical shielding tensor for formaldehyde. It is clear from the above discussion that the accuracy of the ¹⁷O chemical shielding tensor components depends critically on the experimental errors in spin-rotation tensor components. In the case of formaldehyde, the rather inaccurate experimental ¹⁷O spin rotation constants determined in 1965 and 1980 have imposed a severe limitation on the accuracy of the resultant ¹⁷O chemical shielding tensor. Inspection of the individual ¹⁷O spin-rotation tensor components reveals that the accuracy in M_{zz} is not so important to the fitting of the rotational spectra, but crucial to the accuracy of σ_{zz}^p . In particular, while Flygare and Lowe⁴¹ obtained $M_{zz} = -2 \pm 10$ kHz, Cornet et al.⁴² claimed that the contribution of M_{zz} to spectral fitting is negligible so its value was set to zero (i.e., $M_{zz} = 0$ exactly). However, an uncertainty of ± 10 kHz in M_{zz} would introduce an uncertainty in σ_{zz}^p as large as ± 360 ppm according to the first term of eq 6. In this study, in the absence of any new ¹⁷O spin-rotation data, we propose a slightly different approach to improve the accuracy of the ¹⁷O chemical shielding tensor for formaldehyde. First, we follow the procedure of Jameson⁴⁹ to obtain σ_{xx}^{total} and σ_{yy}^{total} by coupling σ_{xx}^p and σ_{yy}^p that are converted from the spin-rotation data reported by Cornet et al.⁴² in 1980 and theoretical values for σ_{xx}^d and σ_{yy}^d .⁶⁴ Second, because the paramagnetic shielding contribution along the direction perpendicular to the H₂C=O plane should be negligibly small, the calculated *total* shielding value along this direction is expected to be reliable to a high degree of accuracy. Thus our approach is to directly use the theoretical σ_{zz}^{total} as the best estimate for an “experimental” value. For this tensor component,

TABLE 3: Computed and Experimental ^{17}O NMR Tensors for Formaldehyde Using Correlation Consistent Basis Sets and Different Methods

method/basis set	δ_{iso} (ppm)	δ_{11} (ppm)	δ_{22} (ppm)	δ_{33} (ppm)	C_Q (MHz) ^a	C_Q (MHz) ^b	η_Q
HF/cc-pVDZ	716.5	1462.8	830.6	-144.0	13.681	12.194	0.582
cc-pVTZ	730.2	1468.8	858.2	-136.4	13.501	12.034	0.668
cc-pVQZ	730.4	1470.6	860.9	-140.4	13.560	12.087	0.662
cc-pV5Z	733.5	1475.0	866.7	-141.2	13.519	12.049	0.662
cc-pV6Z	733.7	1475.1	867.3	-141.1	13.445	11.984	0.663
B3LYP/cc-pVDZ	710.9	1478.8	771.6	-117.6	12.903	12.106	0.590
cc-pVTZ	739.1	1515.0	815.5	-113.2	12.921	12.123	0.691
cc-pVQZ	742.3	1523.4	822.7	-119.2	13.019	12.215	0.690
cc-pV5Z	747.1	1531.3	830.4	-120.6	13.018	12.214	0.689
cc-pV6Z	748.2	1532.9	832.2	-120.6	12.993	12.190	0.686
MP2/cc-pVDZ	582.2	1245.1	642.0	-140.7	13.691	12.631	0.585
cc-pVTZ	621.1	1301.6	698.0	-136.2	13.520	12.474	0.671
cc-pVQZ	730.4	1470.6	860.9	-140.4	13.582	12.531	0.664
cc-pV5Z	733.5	1475.0	866.7	-141.2	13.542	12.493	0.665
cc-pV6Z	619.8	1297.3	705.7	-143.6	13.468	12.426	0.666
exptl.	701 ± 60 ^c	1426 ± 80 ^c	820 ± 80 ^c	-143 ± 5 ^c	12.37 ± 0.01 ^d	12.35 ± 0.01 ^e	0.694 ^d 0.692 ^e

^a Calculated using the standard value of $Q(^{17}\text{O}) = -2.558 \text{ fm}^2$. ^b Calculated using the calibrated values of $Q(^{17}\text{O})$: HF, -2.28; B3LYP, -2.40; MP2, -2.36 fm^2 . For calibrated $Q(^{17}\text{O})$ values, see ref 2. ^c Converted to chemical shifts using the chemical shielding data shown in Table 4 and eq 3. ^d From ref 41. ^e From ref 42.

TABLE 4: Selected Isotropic ^{17}O Chemical Shielding Constants for Formaldehyde Computed with a Variety of Methods

method	basis set	σ_{iso} (ppm)	ref
HF	6-31G(d)	-429.1 ^a	67
	6-311+G(2d,p)	-465.7 ^a	67
	6-311G(d)	-422.7	68
	qz2p	-452.4	46
	pz3d1f	-447.3	46
	[12s8p4d2f]/[8s5p1d]	-441.2	65
	IGLO-III	-415.6	45
	GIAO, tz(2)p	-414.8	45
	cc-pV6Z	-446.2	this work
	DFT	B3LYP/6-31G(d)	-409.5 ^a
B3LYP/6-311+G(2d,p)		-470.9 ^a	67
SOS-DFPT, Loc.3		-430.3	69
B3LYP/cc-pV6Z		-460.7	this work
GIAO/tp		-418.8	70
IGLO/tp		-455.6	70
MP2	qz2p	-333.5	46
	pz3d1f	-337.7	46
	[12s8p4d2f]/[8s5p1d]	-329.8	65
	tz(2)p	-310.2	45
cc-pV6Z	-332.3	this work	
MP3	[12s8p4d2f]/[8s5p1d]	-418.1	65
MP4	qz2p	-371.4	71
L-CCD	[12s8p4d2f]/[8s5p1d]	-418.0	65
CCSD	qz2p	-385.0	46
	pz3d1f	-387.5	46
CCSD(T)	qz2p	-379.1	46
	pz3d1f	-383.1	46

^a Converted to chemical shielding constants from the reported chemical shifts using eq 3.

we expect that the uncertainty is within a few parts per million. Our results are also shown in Table 2. While the errors in σ_{xx} and σ_{yy} are estimated on the basis of the uncertainty in the experimental spin-rotation constants, the error in σ_{zz} is obtained from the estimated residual paramagnetic shielding in this direction. It is interesting to see that, if we use $\sigma_{zz}^{\text{total}} = 431 \text{ ppm}$ and $\sigma_{zz}^{\text{d}} = 475 \text{ ppm}$ to “back-calculate” σ_{zz}^{p} , we get $\sigma_{zz}^{\text{p}} = -44 \text{ ppm}$. This value is between the two values obtained by Flygare and co-workers^{41,47,48} and Jameson.⁴⁹ It is even more comforting to see that, if we use $\sigma_{zz}^{\text{p}} = -44 \text{ ppm}$ and the experimental molecular geometry of formaldehyde to “back-

calculate” M_{zz} using eq 6, we obtain $M_{zz} = -0.8 \text{ kHz}$, which is in excellent agreement with that calculated by Cybulski and Bishop⁶⁵ using a linearized coupled cluster double excitation (L-CCD) method.

Now that we have established a new set of “experimental” ^{17}O chemical shielding tensor components for formaldehyde, we can re-evaluate the accuracy of computational results. We performed extensive computations for the ^{17}O NMR tensors using HF, B3LYP, and MP2 methods and large correlation consistent basis sets. The results are summarized in Table 3. The computed ^{17}O QC tensors are in good agreement with the experimental data. Here we focus our discussion on the computed results for the ^{17}O CS tensor. There is little basis set dependence in the HF results. As expected, results on δ_{33} show an excellent agreement with the “experimental” data. Both δ_{11} and δ_{22} components are greater than the experimental values by ca. 50 ppm. These are surprisingly good results, presumably due to some mutual cancellation of errors. For the B3LYP results, both δ_{22} and δ_{33} are in good agreement with the experimental results, but δ_{11} results appear to be worse than those from the HF calculations. Similarly, little basis set dependence is observed beyond cc-pVTZ. The MP2 results exhibit a stronger dependence on the basis set than the other two methods. With the cc-pV6Z basis set, the computed δ_{11} and δ_{22} components seem to overcompensate for the electron correlation effect. In other words, the MP2 results underestimate the paramagnetic shielding contribution in δ_{11} and δ_{22} components. This effect has been previously observed by Gauss.⁶⁶ We note that Gauss and Stanton⁴⁶ calculated the ^{17}O CS tensor components for formaldehyde at the CCSD(T) level of theory: $\sigma_{11} = -1107.7$, $\sigma_{22} = -469.4$, and $\sigma_{33} = 427.7 \text{ ppm}$. These are in good agreement with the new “experimental” results reported in this study.

For the sake of completeness, we finally come to examine the isotropic ^{17}O chemical shift of formaldehyde, simply because data covering a much greater variety of computational methods are available in the literature. Table 4 gives a summary of the computed isotropic ^{17}O chemical shielding constants for formaldehyde.^{45,46,65,67-71} The general trend is illustrated in Figure 8. Both HF and DFT methods produce results less shielded than the experimental value. The MP2 method clearly

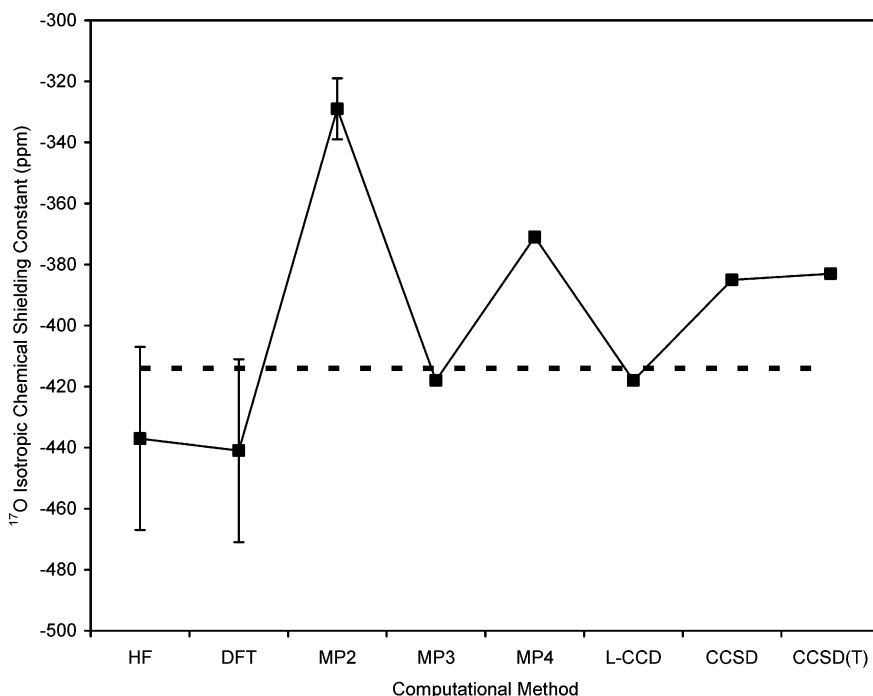


Figure 8. Comparison of calculated and experimental isotropic ^{17}O chemical shielding constants for formaldehyde. The error bars correspond to the ranges of data shown in Table 4. The dotted line indicates the experimental value.

overestimates the electron correlation effect. The oscillatory behavior observed between MP2, MP3, and MP4 values is also typical of a perturbation approach. The overall shape of the curve shown in Figure 8 is quite similar to the trend observed by Gauss and Stanton⁴⁶ for ^{15}N chemical shielding of N_2 . A similar trend has also been observed by Kaupp et al.⁷² in computed ^{17}O chemical shielding constants of ozone. We can conclude that the electron correlation is the common origin in these systems. It appears that CCSD(T) computations give fairly good results compared with the experimental value, bearing in mind the intrinsic uncertainty in the experimental value for formaldehyde.

4. Conclusion

We have experimentally measured the ^{17}O QC and CS tensors for the carbonyl oxygen in *p*-nitro-[1- ^{17}O]benzaldehyde. The results represent the first set of reliable ^{17}O NMR tensor data for the carbonyl oxygen from an aldehyde functional group. Extensive quantum chemical calculations suggest that electron correlation plays a significant role in determining the ^{17}O chemical shielding within the $\text{H}-\text{C}=\text{O}$ plane. We found that, while HF and B3LYP calculations usually underestimate the electron correlation effect, MP2 considerably overestimates its contribution. We have also proposed a new way of constructing an “experimental” ^{17}O chemical shielding tensor for formaldehyde by combining experimental ^{17}O spin-rotation tensor components and theoretical tensor components. A comparison between experimental results and theoretical ones suggests that CCSD(T) results are in reasonable agreement with the experimental values. This indicates that the electron correlation in formaldehyde is well described by the CCSD(T) method.

Acknowledgment. This work was supported by grants from the Natural Sciences and Engineering Research Council (NSERC) of Canada. Quantum mechanical calculations were performed at the High Performance Computing Virtual Laboratory (HPCVL) at Queen’s University. Access to the 900 MHz NMR spectrometer was provided by the National Ultrahigh Field NMR Facility for Solids (Ottawa, Canada), a national research facility funded

by the Canada Foundation for Innovation, the Ontario Innovation Trust, Recherche Québec, NSERC, the National Research Council Canada, and Bruker BioSpin and managed by the University of Ottawa (www.nmr900.ca). We are grateful to Dr. Bing Zhou for providing us with the SIMPSON simulation results and to Professor Cynthia J. Jameson for helpful discussion.

Supporting Information Available: Additional results of the ^{17}O NMR tensors for *p*-nitrobenzaldehyde from quantum chemical calculations (2 tables). Graphic representation of the data shown in Tables 1 and 3 (2 figures). This information is available free of charge via the Internet at <http://pubs.acs.org>.

References and Notes

- (1) Lemaitre, V.; Smith, M. E.; Watts, A. *Solid State Nucl. Magn. Reson.* **2004**, *26*, 215.
- (2) Wu, G. *Progr. Nucl. Magn. Reson. Spectrosc.* **2008**; doi: 10.1016/j.pnmrs.2007.07.004.
- (3) Hu, J.; Chekmenev, E. Y.; Gan, Z.; Gor’kov, P. L.; Saha, S.; Brey, W. W.; Cross, T. A. *J. Am. Chem. Soc.* **2005**, *127*, 11922.
- (4) Chekmenev, E. Y.; Waddell, K. W.; Hu, J.; Gan, Z.; Wittebort, R. J.; Cross, T. A. *J. Am. Chem. Soc.* **2006**, *128*, 9849.
- (5) Kwan, I. C. M.; Mo, X.; Wu, G. *J. Am. Chem. Soc.* **2007**, *129*, 2398.
- (6) Wu, G.; Yamada, K. *Solid State Nucl. Magn. Reson.* **2003**, *24*, 196.
- (7) Wong, A.; Thurgood, G.; Dupree, R.; Smith, M. E. *Chem. Phys.* **2007**, *337*, 144.
- (8) Wu, G.; Yamada, K.; Dong, S.; Grondey, H. *J. Am. Chem. Soc.* **2000**, *122*, 4215.
- (9) Yamada, K.; Dong, S.; Wu, G. *J. Am. Chem. Soc.* **2000**, *122*, 11602.
- (10) Dong, S.; Ida, R.; Wu, G. *J. Phys. Chem. A* **2000**, *104*, 11194.
- (11) Dong, S.; Yamada, K.; Wu, G. *Z. Naturforsch. A* **2000**, *55*, 21.
- (12) Wu, G.; Hook, A.; Dong, S.; Yamada, K. *J. Phys. Chem. A* **2000**, *104*, 4102.
- (13) Wu, G.; Dong, S. *Chem. Phys. Lett.* **2001**, *334*, 265.
- (14) Wu, G.; Dong, S. *J. Am. Chem. Soc.* **2001**, *123*, 9119.
- (15) Wu, G.; Dong, S.; Ida, R. *Chem. Commun.* **2001**, 891.
- (16) Wu, G.; Dong, S.; Ida, R.; Reen, N. *J. Am. Chem. Soc.* **2002**, *124*, 1768.
- (17) Park, K. D.; Guo, K.; Adebodun, F.; Chiu, M. L.; Sligar, S. G.; Oldfield, E. *Biochemistry* **1991**, *30*, 2333.

- (18) Oldfield, E.; Lee, H. C.; Coretsopoulos, C.; Adebodun, F.; Park, K. D.; Yang, S. T.; Chung, J.; Phillips, B. *J. Am. Chem. Soc.* **1991**, *113*, 8680.
- (19) Kuroki, S.; Takahashi, A.; Ando, I.; Shoji, A.; Ozaki, T. *J. Mol. Struct.* **1994**, *323*, 197.
- (20) Takahashi, A.; Kuroki, S.; Ando, I.; Ozaki, T.; Shoji, A. *J. Mol. Struct.* **1998**, *442*, 195.
- (21) McMahon, M. T.; deDios, A. C.; Godbout, N.; Salzmman, R.; Laws, D. D.; Le, H. B.; Havlin, R. H.; Oldfield, E. *J. Am. Chem. Soc.* **1998**, *120*, 4784.
- (22) Salzmman, R.; Ziegler, C. J.; Godbout, N.; McMahon, M. T.; Suslick, K. S.; Oldfield, E. *J. Am. Chem. Soc.* **1998**, *120*, 11323.
- (23) Yamauchi, K.; Kuroki, S.; Ando, I.; Ozaki, T.; Shoji, A. *Chem. Phys. Lett.* **1999**, *302*, 331.
- (24) Salzmman, R.; McMahon, M. T.; Godbout, N.; Sanders, L. K.; Wojdelski, M.; Oldfield, E. *J. Am. Chem. Soc.* **1999**, *121*, 3818.
- (25) Godbout, N.; Sanders, L. K.; Salzmman, R.; Havlin, R. H.; Wojdelski, M.; Oldfield, E. *J. Am. Chem. Soc.* **1999**, *121*, 3829.
- (26) Yamauchi, K.; Kuroki, S.; Ando, I. *J. Mol. Struct.* **2002**, *602*, 171.
- (27) Pike, K. J.; Lemaitre, V.; Kukul, A.; Anupold, T.; Samoson, A.; Howes, A. P.; Watts, A.; Smith, M. E.; Dupree, R. *J. Phys. Chem. B* **2004**, *108*, 9256.
- (28) Wong, A.; Pike, K. J.; Jenkins, R.; Clarkson, G. J.; Anupold, T.; Howes, A. P.; Crout, D. H. G.; Samoson, A.; Dupree, R.; Smith, M. E. *J. Phys. Chem. A* **2006**, *110*, 1824.
- (29) Wong, A.; Howes, A. P.; Pike, K. J.; Lemaitre, V.; Watts, A.; Anupold, T.; Past, J.; Samoson, A.; Dupree, R.; Smith, M. E. *J. Am. Chem. Soc.* **2006**, *128*, 7744.
- (30) Chekmenev, E. Y.; Gor'kov, P. L.; Cross, T. A.; Alaouie, A. M.; Smirnov, A. I. *Biophys. J.* **2006**, *91*, 3076.
- (31) Howes, A. P.; Anupold, T.; Lemaitre, V.; Kukul, A.; Watts, A.; Samoson, A.; Smith, M. E.; Dupree, R. *Chem. Phys. Lett.* **2006**, *421*, 42.
- (32) Lemaitre, V.; De Planque, M. R. R.; Howes, A. P.; Smith, M. E.; Dupree, R.; Watts, A. *J. Am. Chem. Soc.* **2004**, *126*, 15320.
- (33) Lemaitre, V.; Pike, K. J.; Watts, A.; Anupold, T.; Samoson, A.; Smith, M. E.; Dupree, R. *Chem. Phys. Lett.* **2003**, *371*, 91.
- (34) Waddell, K. W.; Chekmenev, E. Y.; Wittebort, R. J. *J. Phys. Chem. B* **2006**, *110*, 22935.
- (35) van Beek, J. D.; Dupree, R.; Levitt, M. H. *J. Magn. Reson.* **2006**, *179*, 38.
- (36) Brinkmann, A.; Kentgens, A. P. M. *J. Am. Chem. Soc.* **2006**, *128*, 14758.
- (37) Brinkmann, A.; Kentgens, A. P. M. *J. Phys. Chem. B* **2006**, *110*, 16089.
- (38) Gullion, T.; Yamauchi, K.; Okonogi, M.; Asakura, T. *Macromolecules* **2007**, *40*, 1363.
- (39) Sefzik, T. H.; Houseknecht, J. B.; Clark, T. M.; Prasad, S.; Lowary, T. L.; Gan, Z.; Grandinetti, P. *J. Chem. Phys. Lett.* **2007**, *434*, 312.
- (40) Cheng, C. P.; Brown, T. L. *J. Am. Chem. Soc.* **1979**, *101*, 2327.
- (41) Flygare, W. H.; Lowe, J. T. *J. Chem. Phys.* **1965**, *43*, 3645.
- (42) Cornet, R.; Landsberg, B. M.; Winnawisser, G. *J. Mol. Spectrosc.* **1980**, *82*, 253.
- (43) Jackisch, M. A.; Fronczek, F. R.; Butler, L. G. *Acta Cryst.* **1989**, *C45*, 2016.
- (44) King, Jr, J. A.; Bryant, Jr, G. L. *Acta Cryst.* **1996**, *C52*, 1691.
- (45) Fleischer, U.; van Wullen, C.; Kutzelnigg, W. NMR chemical shift computation: Ab initio. In *Encyclopedia of Nuclear Magnetic Resonance*; Grant, D. M., Harris, R. K., Eds.; Wiley: New York, 1996; p 1827.
- (46) Gauss, J.; Stanton, J. F. *J. Chem. Phys.* **1996**, *104*, 2574.
- (47) Gierke, T. D.; Flygare, W. H. *J. Am. Chem. Soc.* **1972**, *94*, 7277.
- (48) Flygare, W. H. *Chem. Rev.* **1974**, *74*, 653.
- (49) Jameson, C. J. In *Specialist Periodical Reports*; Webb, G. A., Ed.; Royal Society of Chemistry: London, UK, 1989; Vol. 18, pp 1–33, Chapter 1.
- (50) Frisch, M. J.; Trucks, G. W.; Schlegel, H. B.; Scuseria, G. E.; Robb, M. A.; Cheeseman, J. R.; Montgomery, J., J. A.; Vreven, T.; Kudin, K. N.; Burant, J. C.; Millam, J. M.; Iyengar, S. S.; Tomasi, J.; Barone, V.; Mennucci, B.; Cossi, M.; Scalmani, G.; Rega, N.; Petersson, G. A.; Nakatsuji, H.; Hada, M.; Ehara, M.; Toyota, K.; Fukuda, R.; Hasegawa, J.; Ishida, M.; Nakajima, T.; Honda, Y.; Kitao, O.; Nakai, H.; Klene, M.; Li, X.; Knox, J. E.; Hratchian, H. P.; Cross, J. B.; Bakken, V.; Adamo, C.; Jaramillo, J.; Gomperts, R.; Stratmann, R. E.; Yazyev, O.; Austin, A. J.; Cammi, R.; Pomelli, C.; Ochterski, J. W.; Ayala, P. Y.; Morokuma, K.; Voth, G. A.; Salvador, P.; Dannenberg, J. J.; Zakrzewski, V. G.; Dapprich, S.; Daniels, A. D.; Strain, M. C.; Farkas, O.; Malick, D. K.; Rabuck, A. D.; Raghavachari, K.; Foresman, J. B.; Ortiz, J. V.; Cui, Q.; Baboul, A. G.; Clifford, S.; Cioslowski, J.; Stefanov, B. B.; Liu, G.; Liashenko, A.; Piskorz, P.; Komaromi, I.; Martin, R. L.; Fox, D. J.; Keith, T.; Al-Laham, M. A.; Peng, C. Y.; Nanayakkara, A.; Challacombe, M.; Gill, P. M. W.; Johnson, B.; Chen, W.; Wong, M. W.; Gonzalez, C.; Pople, J. A. *Gaussian 03*, revision C.02; Gaussian, Inc.: Wallingford, CT, 2004.
- (51) *SHELXTL Crystal Structure Analysis Package*, version 5 ed.; Bruker Analytical X-ray System, Siemens: Madison, WI, 1995.
- (52) Oka, T. *J. Phys. Soc. Jpn.* **1960**, *15*, 2274.
- (53) Pyykko, P. *Mol. Phys.* **2001**, *99*, 1617.
- (54) Wasylshen, R. E.; Bryce, D. L. *J. Chem. Phys.* **2002**, *117*, 10061.
- (55) Scheubel, W.; Zimmermann, H.; Haebleren, U. *J. Magn. Reson.* **1985**, *63*, 544.
- (56) Gready, J. E. *J. Am. Chem. Soc.* **1981**, *103*, 3682.
- (57) Gready, J. E. *J. Phys. Chem.* **1984**, *88*, 3497.
- (58) Keith, T. A.; Bader, R. F. W. *Chem. Phys. Lett.* **1992**, *194*, 1.
- (59) Keith, T. A.; Bader, R. F. W. *Chem. Phys. Lett.* **1993**, *210*, 223.
- (60) Cheeseman, J. R.; Frisch, M. J.; Trucks, G. W.; Keith, T. A. *J. Chem. Phys.* **1996**, *104*, 5497.
- (61) Ramsey, N. F. *Phys. Rev.* **1950**, *78*, 699.
- (62) Flygare, W. H. *J. Chem. Phys.* **1964**, *41*, 793.
- (63) *Quantities, Units and Symbols in Physical Chemistry*, 2nd ed.; Mills, I., Cvitas, T., Homann, K., Kallay, N., Kuchitsu, K., Eds.; Blackwell Science: Oxford, 1993.
- (64) Neumann, D. B.; Moskowitz, J. W. *J. Chem. Phys.* **1969**, *50*, 2216.
- (65) Cybulski, S. M.; Bishop, D. M. *J. Chem. Phys.* **1997**, *106*, 4082.
- (66) Gauss, J. *J. Chem. Phys.* **1993**, *99*, 3629.
- (67) Cheeseman, J. R.; Trucks, G. W.; Keith, T. A.; Frisch, M. J. *J. Chem. Phys.* **1996**, *104*, 5497.
- (68) Chesnut, D. B.; Phung, C. G. *J. Chem. Phys.* **1989**, *91*, 6238.
- (69) Fadda, E.; Casida, M. E.; Salahub, D. R. *J. Chem. Phys.* **2003**, *118*, 6758.
- (70) Schreckenbach, G.; Ziegler, T. *J. Phys. Chem.* **1995**, *99*, 606.
- (71) Gauss, J.; Stanton, J. F. *J. Chem. Phys.* **1995**, *103*, 3561.
- (72) Kaupp, M.; Malkina, O. L.; Malkin, V. G. *J. Chem. Phys.* **1997**, *106*, 9201.